Contents lists available at SCCE

Journal of Soft Computing in Civil Engineering

Journal homepage: www.jsoftcivil.com

# Optimizing Reinforced Concrete Cantilever Retaining Walls Using Gases Brownian Motion Algorithm (GBMOA)

**M. Shalchi Tousi[1], M. Ghazavi[2], S. Laali[3*]**

1. Engineer, Department of Civil Engineering Faculty of Central Tehran Branch, Islamic Azad University, Tehran, Iran
2. Professor, Faculty of Civil Engineering KN Toosi University of Technology, Tehran, Iran
3. Engineer, Department of Civil Engineering, University of Science and Culture, Tehran, Iran

Corresponding author: *laali.smn@gmail.com*

https://doi.org/10.22115/SCCE.2021.248638.1256

## ARTICLE INFO

Article history:
Received: 16 September 2020
Revised: 12 January 2021
Accepted: 14 January 2021

Keywords:
Retaining wall optimization;
Sensitivity analysis;
Gasses Brownian motion optimization;
Cost and weight objective functions.

## ABSTRACT

In this paper, the cost and weight of the reinforcement concrete cantilever retaining wall are optimized using Gases Brownian Motion Optimization Algorithm (GBMOA) which is based on the gas molecules motion. To investigate the optimization capability of the GBMOA, two objective functions of cost and weight are considered and verification is made using two available solutions for retaining wall design. Furthermore, the effect of wall geometries of retaining walls on their cost and weight is investigated using four different T-shape walls. Besides, sensitivity analyses for effects of backfill slope, stem height, surcharge, and backfill unit weight are carried out and of soil. Moreover, Rankine and Coulomb methods for lateral earth pressure calculation are used and results are compared. The GBMOA predictions are compared with those available in the literature. It has been shown that the use of GBMOA results in reducing significantly the cost and weight of retaining walls. In addition, the Coulomb lateral earth pressure can reduce the cost and weight of retaining walls.

How to cite this article: Shalchi Tousi M, Ghazavi M, Laali S. Optimizing reinforced concrete cantilever retaining walls using gases brownian motion algorithm (GBMOA). J Soft Comput Civ Eng 2021;5(1):01–18. https://doi.org/10.22115/scce.2021.248638.1256.

# 1. Introduction

Retaining walls supporting backfill are used widely practice and thus must meet stable against sliding, and overturning. Besides, they must be designed on a soil bed having sufficient bearing capacity and limited settlement, and also must meet structural requirements. The design of such walls should be such that the cost and weight of walls become minimized. Thus, it has been tried to use theories to optimize these walls. These theories include nonlinear programming (Saribas and Erbatur, 1996) [1], simulated annealing optimization (Sivakumar and Munwar, 1999 [2]; Yepes et al., 2008 [3]), target reliability approach (Ceranic and Freyre, 2008) [4], ant colony optimization algorithm (Ghazavi and Bazzazian, 2011) [5], bacterial foraging optimization algorithm (Ghazavi and Salavati, 2011) [6], and charged system search algorithm (Kaveh and Behnam, 2013) [7].

Despite comprehensive progress achieved in optimizing retaining walls from structural and geotechnical viewpoints, in the literature, it is still felt to research this scenario. In this paper, a relatively new algorithm called the gasses Brownian motion algorithm optimization (GBMOA) developed by Abdechiri (2013) [8] is used to optimize the design of retaining walls from viewpoints of cost and weight, which are considered as objective functions.

The GBMOA first presented by Abdechiri (2013) [8] considers the fast movement of molecules in their spaces and emit in the total space quickly. This algorithm is based on the Brownian motion and turbulent rotational motion of ingredient in their locations. The local search and global search in this algorithm are made by using Brownian motion and turbulent rotational motion of each molecule. The use of these features of gas's molecules and by modeming their factional motion, the GBMOA may be a powerful tool for optimization.

In this paper, the GBMOA is used for retaining wall optimization and the results are compared with those presented by Saribas and Erbatur (1996) [1] who performed sensitivity analyses for stem height, backfill slope, and surcharge load. At the first section, the GBMOA performance is proved by comparing the obtained objective functions and variables optimum values with results of Saribas and Erbatur (1996) [1]. Then the variation influence of constant parameters is investigated such as stem height, surcharge load, etc. They concluded that by increasing the stem height and surcharge, the cost and weight objective functions increase. Moreover, by increasing the backfill slope value from $0^o$ to $20^o$, the cost and weight of the wall first decrease and then increase. In addition, the optimized predicted data obtained from the GBMOA are compared with those obtained from conventional design (Bowles, 1982) [9]. The obtained results show that the GBMOA in comparison with conventional design can reduce the wall cost and weight about %42.14 and %45.14, respectively. At the next section, four different T-shape walls are considered to investigate the effect of wall geometries on their costs and weights. Researches are done to show that the wall with the lowest cost isn't lead to the lowest weight for the wall. Furthermore, effects of primary and fix parameters on objective functions are investigated by performing sensitivity analysis on four factors including backfill slope, retained soil unit weight and backfill internal friction angle, surcharge load and wall stem height. Finally, the application of Coulomb and Rankine methods on the calculation of the lateral earth pressure is studied. The

results show that the Coulomb method reduces the cost and weight objective function in both two types of wall. In other words, using Coulomb method for the design of concrete cantilever retaining walls can lead to better results in comparison with Rankine method.

## 2. Introduction of gases Brownian motion algorithm

The GBMOA has been presented based on the ideal gas low, molecules characteristics, and gases motion models. Equation $PV = nRT$ is used in the ideal gas in which $P$, $V$, $n$, $R$ and $T$ are the absolute pressure, the system volume, the number of particles in the gas, the gasses world instant and the system temperature based on Kelvin, respectively. The speed of gas molecule with the mass of $m$ is equal to $v = \sqrt{3kT/m}$ which leads to the motion of molecules randomly in time. It is important to note that the environment temperature has the most influence on the irregular and Brownian motions. By decreasing the environment temperature to zero, the system will be stable. As a result, the motion speed of each molecule will be zero. Therefore, the stability of this system is made at $T = 0$ temperature. The gas molecules consist of turbulent rotational motion in their location in addition to Brownian motion. In this algorithm, the modelling of both above-mentioned motions is considered.

Due to the Brownian nature of the gas molecule motions, there is no direct line for speeding of molecules. As a result, they will move irregularly in different lines. In addition, the line and speed of the molecules will change due to their confliction with one another. This causes different speeds for gas molecules. The step by step procedure of this algorithm is:

1- According to the accuracy of the process and the required time to perform the program, the desired numbers of gas molecules will be made accidentally. By increasing the number of molecules, the accuracy of the process increases.
2- The turbulence radius for each molecule in the interval of [0, 1] are randomly considered.
3- Then, the temperature is selected for this system, leading to convergence of the algorithm.

At the first step, the value of temperature is too high and it decreases during the operating of the algorithm. This process will be stopped while the temperature is equal to zero. In addition, at the beginning of the process, the molecules will search the wide range that is called global search. This is made because of the high value of kinetic energy and speed. After some times and by decreasing the temperature, kinetic energy and the speed of the molecules, the local search will be made (Figure 1).

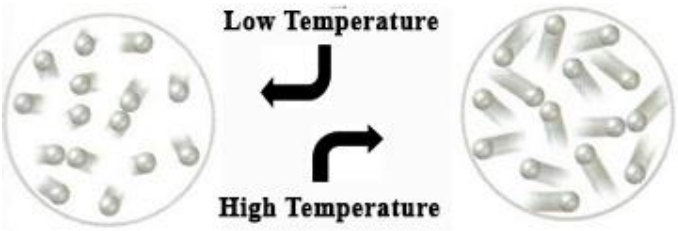


**Fig. 1.** Effect of reducing temperature of kinetic energy.

4- The updating of the speed and location of the molecules are calculated as:

$$v_t = v_{t-1} + \sqrt{\frac{3kT}{m}} \quad (1)$$

$$x_t = x_{t-1} + v_t \quad (2)$$

where v is the velocity of the molecules, x=location of the molecules, m=mass, T=temperature in Kelvin, and K=Kelvin constant equals $1.38 \times 10^{-23}$.

5- The obtained results are evaluated using a fitness function. The best answers are maintained for comparison with other obtained results. If the obtained results cannot gratify the constraints, they will be penalized by the penalty functions.

6- Each molecule vibrates in their locations and in the specified radius, in addition, to move in different directions. The process of the local search at the first step and global search in the last steps are made by this vibration. The location of each molecule is:

$$\theta_{n+1} = \theta_n + b - \left({}^{a}/_{2\pi}\right) \sin(2\pi\theta_n) \bmod(1) \quad (3)$$

where θ is vibration and a=0.5 and b=0.2.

7- As same as step 5, the fitness function is recalled again and the best answers are maintained. Moreover, if obtained results cannot gratify the constraints, they will be penalized by the penalty functions.

8- The algorithm will be stopped while the temperature decreases to zero, otherwise the search will be continued.

In this algorithm, the global and local searches are performed by using molecules turbulent rotational and Brownian motions that are shown in Figure 2. As shown, gas molecules are moved irregularly and in random line. In addition, they will move in their location by vibrations.

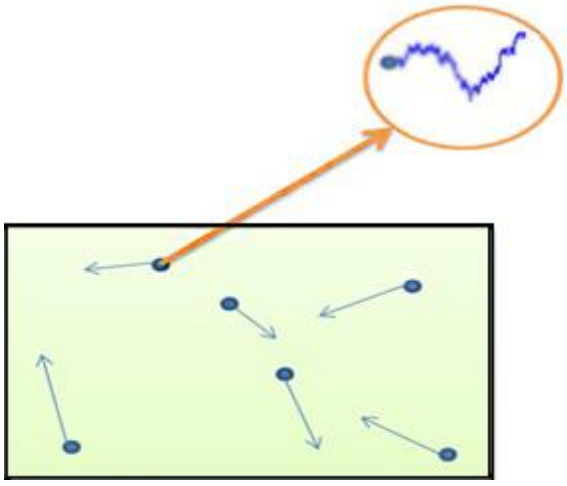

**Fig. 2.** Molecules Brownian and turbulent rotational motion in the search space.

## 3. The Parameters and requirements for retaining wall optimization

A retaining wall shown in Figure 3 is considered for the current study.

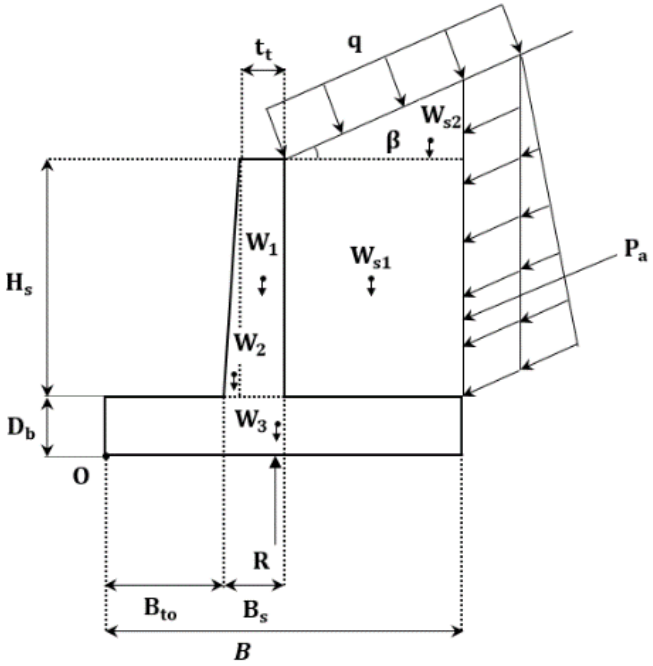


**Fig. 3.** Geometry of retaining wall.

### 3.1. Design of variables

In this section, wall dimensions, the required steel value, the concrete compressive strength ($F_c$), yield strength of steel ($F_y$), and steel bar diameter ($d_b$) are presented as variables (Table 1). It should be noted that the number of required bars for stem, toe, and heel is as the software output by applying minimum and maximum values based on the American Concrete Institute Code (ACI-2008) [10]. The discrete values for the decision variables are defined as bellow:

$$\mathrm{Fy} = 350, 400, 500 \text{ MPa} \tag{4}$$

$$\mathrm{Fc} = 21, 24, 28, 35, 42, 45 \text{ MPa} \tag{5}$$

$$\mathrm{d_b} = 10, 12, 14, 16, 18, 20, 22, 24, 26 \text{ mm} \tag{6}$$

It is clear that all continuous variables presented in Table 2 consist of upper and lower bounds. Parameter $H_s$ as a primary input data is the wall stem height (Table 2). Some primary values are assumed for the required steel area. The maximum and minimum values are controlled based on the ACI code [10] considering constraints. The zero value for the lower limit of the area is selected due to no necessity to compressive steel. In other words, if the tension steel is sufficient for the applied moment, zero compressive steel is obtained.

**Table 1**
Variables and output software for retaining wall design.

| Groups | Name | Unit | Symbol | Type |
|---|---|---|---|---|
| **Variables of geometrical specification of wall** | Total base width | m | B | Continuous |
| | Toe width | | $B_{to}$ | |
| | Stem thickness at bottom | | $B_s$ | |
| | Thickness of base | | $D_b$ | |
| | Stem thickness at Top | | $t_t$ | |
| **Variables of specification of used steels** | Stem tensile steel area | $cm^2/m$ | AstS | Continuous |
| | Toe tensile steel area | | AstT | |
| | Heel tensile steel area | | AstH | |
| | Stem compressive steel area | | AscS | |
| | Toe compressive steel area | | AscT | |
| | Heel compressive steel area | | AscH | |
| | Yield strength of stem tensile steel | MPa | $F_{y_1}$ | discrete |
| | Yield strength of stem compressive steel | | $F_{y_2}$ | |
| | Yield strength of toe tensile steel | | $F_{y_3}$ | |
| | Yield strength of toe compressive steel | | $F_{y_4}$ | |
| | Yield strength of heel tensile steel | | $F_{y_5}$ | |
| | Yield strength of heel compressive steel | | $F_{y_6}$ | |
| | Steel bar diameter | mm | $d_b$ | |
| **Variables of specification of concrete** | Compressive strength of stem concrete | MPa | $F_{c_s}$ | discrete |
| | Compressive strength of base concrete | | $F_{c_f}$ | |
| **Software output** | Number of stem tensile steel | – | $n_1$ | discrete |
| | Number of toe tensile steel | | $n_2$ | |
| | Number of heel tensile steel | | $n_3$ | |
| | Number of stem compressive steel | | $n_4$ | |
| | Number of toe compressive steel | | $n_5$ | |
| | Number of heel compressive steel | | $n_6$ | |

**Table 2**
Lower and upper bounds for continuous variables.

| Variable name | Unit | Lower bound | Upper bound |
|---|---|---|---|
| **Total base width** | m | $(24 \times H_s)/55$ | $(7 \times H_s)/9$ |
| **Toe width** | m | $(8 \times H_s)/55$ | $(7 \times H_s)/27$ |
| **Stem thickness at bottom** | m | 0.2 | $H_s/9$ |
| **Thickness of base** | m | $H_s/11$ | $H_s/9$ |
| **Stem thickness at top** | m | 0.2 | 0.3 |
| **Area of tensile and compressive steel** | $cm^2/m$ | 0 | 80 |

## 3.2. Objective functions

The cost and weight functions are considered as objective functions. The main aim of optimization is determining the dimensions and characteristics of the wall by considering structural and geotechnical constraints with the lowest cost and weight values. It is important to note that for the calculation of the required steel weight and the required development length of bars in tension or compression ($l_{dh}$, $l_{dc}$) is considered based on ACI Code (2008) [10]. The objective functions are defined by:

$$f(C) = C_s W_s + C_c V_c \quad (7)$$

$$f(W) = W_s + 100 V_c \gamma_c \quad (8)$$

where $C_s$ is the cost of steel ($/kg), $C_c$ is the cost of concrete ($/m$^3$) for formatting, concretion, vibration and the human cost, $W_{st}$ is the steel weight in the wall length unit (kg), $V_c$ is the concrete volume in the wall length unit ($m^3$), and $\gamma_c$ is the weight of the concrete unit ($kN/m^3$).

### 3.3. Design constraints

In the design of retaining walls, some requirements are necessary to avoid structural and geotechnical failure. As a result, these requirements which control design variables are known as constraints. In optimization algorithms, constraints are shown by g satisfy:

$$g_i(x) \leq 0 \ , \ i = 1,2, \dots, m \quad (9)$$

where m is the number of constraints shown in Table 3.

In addition, Rankine and Hansen methods are used to calculate the lateral earth pressure and bearing capacity, respectively.

**Table 3**
Constraints for retaining wall design.

| Name of constraint | Unit | Comments |
|---|---|---|
| Overturning stability | kN. m | $\frac{M_r}{M_o} \geq SF_o \ \rightarrow \ (M_o \times SF_o) - M_r \leq 0$ |
| Sliding stability | kN | $\frac{F_r + P_p}{P_{ah}} \geq SF_s \quad \rightarrow \quad (P_{ah} \times SF_s) - (F_r + P_p) \leq 0$ |
| No tension condition in foundation | m | $e \leq \frac{B}{6} \quad \rightarrow \quad e - \frac{B}{6} \leq 0$ |
| Bearing capacity | kPa | $\frac{q_{ult}}{q_{max}} \geq SF_b \quad \rightarrow \quad (q_{max} \times SF_b) - q_{ult} \leq 0$ |
| Shear control | kN | $V_n \times \emptyset_V \geq V_u \quad \rightarrow \quad V_u - (V_n \times \emptyset_V) \leq 0$<br>$V_n = \frac{1}{6}\sqrt{\acute{f}_c} d$ |
| Moment control | kN. m | $M_n \times \emptyset_M \geq M_u \quad \rightarrow \quad M_u - (M_n \times \emptyset_M) \leq 0$ |
| Minimum of tensile steel | – | $A_s \geq A_{s_{min}} \quad \rightarrow \quad A_{s_{min}} - A_s \leq 0$<br>$A_{s_{min}} = max\left(\frac{0.25bd\sqrt{\acute{f}_c}}{F_y}, \frac{1.4bd}{F_y}\right)$ |
| Maximum of tensile steel | – | $\rho \leq \rho_{max}$ |
| Yielding of tensile steel | – | $\rho \leq \rho_b$ |
| Yielding of compressive steel | – | $\rho \geq \overline{\rho_{min}}$ |
| Minimum Footing depth | m | $d \geq d_{min}$ |
| Stem slope control | – | $tan\,\alpha \geq 0.02$ |
| Minimum distance of tensile steel | m | $L_b \geq max(2.5cm, d_b)$ |
| Minimum distance of compressive steel | m | $L_b \geq max(2.5cm, d_b)$ |
| Maximum distance of tensile steel | m | Stem: $L_b \leq \min(45.72cm, 3B_s)$,<br>toe and heel: $L_b \leq \min(45.72cm, 3D_b)$ |

# 4. Verification

To monitor the ability of the GBMOA, its predicted results are compared with those presented by Saribas and Erbatur (1996) [1] and also with conventional design mentioned by Bowles (1982) [9]. Saribas and Erbatur (1996) [1] used a nonlinear programming method for concrete wall optimization from weight and cost viewpoints. They considered T-shape walls with varying stem thickness. Table 4 shows all constant parameters such as the height of the wall for two different examples. The required variables and constraints of structural and geotechnical are shown in Table 5.

**Table 4**
Constant parameters for retaining wall.

| Parameter | Symbol | Example 1 | Example 2 |
|---|---|---|---|
| Height of stem (m) | $H_s$ | 3 | 4.5 |
| Stem thickness at the top (m) | $t_t$ | 0.2 | 0.25 |
| Yield strength of reinforcing steel (MPa) | $F_y$ | 400 | 400 |
| Compressive strength of concrete (MPa) | $f_c^{'}$ | 21 | 21 |
| Concrete cover (cm) | $d_{co}$ | 7 | 7 |
| Maximum steel percentage | $\rho_{max}$ | 0.016 | 0.016 |
| Minimum steel percentage | $\rho_{min}$ | 0.00333 | 0.00333 |
| Shrinkage and temporary reinforcement percent | $\rho_{st}$ | 0.002 | 0.002 |
| Diameter of bar (cm) | $\phi_{bar}$ | 1.2 | 1.4 |
| Surcharge load (kPa) | $q$ | 20 | 30 |
| Backfill slope (Degree) | $\beta$ | 10 | 15 |
| Internal friction angle of retained soil (Degree) | $\phi$ | 36 | 36 |
| Internal friction angle of base soil (Degree) | $\acute{\phi}$ | 0 | 34 |
| Unit weight of retained soil ($kN/m^3$) | $\gamma_s$ | 17.5 | 17.5 |
| Unit weight of base soil ($kN/m^3$) | $\acute{\gamma_s}$ | 18.5 | 18.5 |
| Unit weight of concrete ($kN/m^3$) | $\gamma_c$ | 23.5 | 23.5 |
| Cohesion of base soil (kPa) | $c$ | 125 | 100 |
| Design load factor | LF | 1.7 | 1.7 |
| Depth of soil in front of wall (m) | $D_f$ | 0.5 | 0.75 |
| Cost of steel ($/kg) | $C_s$ | 0.4 | 0.4 |
| Cost of concrete ($/$m^3$) | $C_c$ | 40 | 40 |
| Factor of safety against sliding | $SF_s$ | 1.5 | 1.5 |
| Factor of safety for overturning stability | $SF_o$ | 1.5 | 1.5 |
| Factor of safety for bearing capacity | $SF_b$ | 3 | 3 |

**Table 5.**
Variables and constraints

| Variables | Constraints |
|---|---|
| Total base width | Shear at bottom of stem |
| Toe width | Moment at bottom of stem |
| Stem thickness at bottom | Overturning stability |
| Thickness of base | Sliding stability |
| Area of stem tensile steel | No tension condition in foundation |
| Area of toe tensile steel | Bearing capacity |
| Area of heel tensile steel | Toe shear |
| | Toe moment |
| | Heel shear |
| | Heel moment |

Table 6 compares results obtained from the GBMOA and those reported by three optimization methods, which are RETOPT (Saribas and Erbatur, 1996) [1]; ant colony optimization (ACO) algorithm (Ghazavi and Bazzazian, 2011) [5], and bacterial foraging optimization (BFOA) algorithm (Ghazavi and Salavati, 2011) [6]. As seen, the GMBOA objective function output data agree well other methods especially with the presented by Saribas and Erbatur (1996) [1].

Table 7 compares the optimum values of variables and constraints at optimum points predicted by the GBMOA and those of Saribas and Erbatur (1996) [1]. The obtained results and the values close to Saribas's numbers show that the GBMOA method has a perfect performance.

**Table 6**
Comparison of results predicted by GBMOA (present study), ACO (Ghazavi and Bazzazian, 2011) [5], BFOA (Ghazavi and Salavati 2011) [6], and RETOPT Saribus and Erbatur (1996) [1].

| Objective function | Saribas minimum value (RETOPT) | Minimum value of GBMOA | Minimum value of BFOA | Minimum value of ACO | Difference between Minimum value of Saribas and GBMOA | Difference between Minimum value of Saribas and ACO | Difference between Minimum value of Saribas and BFOA |
|---|---|---|---|---|---|---|---|
| Example 1 | | | | | | | |
| **Cost ($/m)** | 82.474 | 82.922 | – | – | %0.543 | - | - |
| **Weight (Kg/m)** | 2498.7 | 2500 | – | – | %0.052 | - | - |
| Example 2 | | | | | | | |
| **Cost ($/m)** | 189.546 | 189.556 | 190.574 | 201.185 | %0.005 | %6.140 | %0.542 |
| **Weight (Kg/m)** | 5280 | 5282 | 5343.221 | 5540.3 | %0.038 | %4.929 | \|%1.197 |

**Table 7**
Optimum values of variables and constraints at optimum points predicted by GBMOA and Saribus and Erbatur (1996) [1].

| Design variables | | Optimum values for minimum cost | | Optimum values for minimum weight | |
|---|---|---|---|---|---|
| | | Saribas (RETOPT) | GBMOA algorithm | Saribas (RETOPT) | GBMOA algorithm |
| Example 1 | | | | | |
| $X_1$ | Total base width (m) | 1.578 | 1.578 | 1.574 | 1.574 |
| $X_2$ | Toe width (m) | 0.436 | 0.436 | 0.441 | 0.459 |
| $X_3$ | Stem thickness at the bottom (m) | 0.258 | 0.259 | 0.200 | 0.200 |
| $X_4$ | Thickness of base (m) | 0.273 | 0.2727 | 0.273 | 0.2727 |
| $X_5$ | Area of stem tensile steel ($cm^2/m$) | 12.574 | 12.482 | 21.072 | 21.079 |
| $X_6$ | Area of toe tensile steel ($cm^2/m$) | 6.551 | 6.551 | 6.551 | 6.551 |
| $X_7$ | Area of heel tensile steel ($cm^2/m$) | 6.551 | 6.551 | 6.681 | 6.559 |
| Example 2 | | | | | |
| $X_1$ | Total base width (m) | 2.254 | 2.254 | 2.238 | 2.238 |
| $X_2$ | Toe width (m) | 0.655 | 0.654 | 0.655 | 0.654 |
| $X_3$ | Stem thickness at the bottom (m) | 0.417 | 0.418 | 0.300 | 0.300 |
| $X_4$ | Thickness of base (m) | 0.409 | 0.409 | 0.409 | 0.409 |
| $X_5$ | Area of stem tensile steel ($cm^2/m$) | 23.475 | 23.379 | 41.626 | 41.610 |
| $X_6$ | Area of toe tensile steel ($cm^2/m$) | 11.059 | 11.058 | 11.059 | 11.058 |
| $X_7$ | Area of heel tensile steel ($cm^2/m$) | 11.059 | 11.058 | 11.059 | 11.058 |

As the second verification, a T-shape wall shown in Figure 4 is considered and designed with the GBMOA and conventional design method (Bowles, 1982) [9]. The primary and constant parameters are summarized in Table 8. The results show that the wall optimization results in about %42.14 and %45.14 the cost and weight reduction, respectively, compared with those obtained from conventional manual design (Table 9). The optimum values of variables are shown in tables 10.

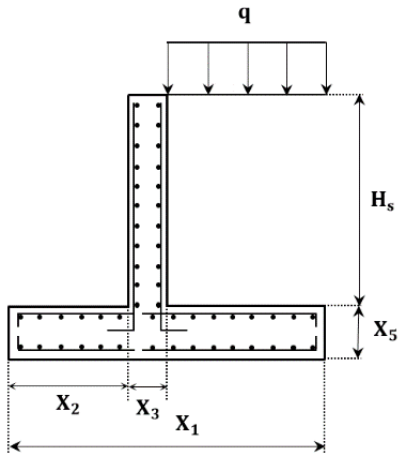


**Fig. 4.** Wall model used for second verification case.

**Table 8**
Design parameters for second verification case.

| parameter | symbol | value |
|---|---|---|
| Height of stem (m) | $H_s$ | 2.44 |
| Concrete cover (cm) | $d_{co}$ | 5 |
| Shrinkage and temporary reinforcement percent | $\rho_{st}$ | 0.0018 |
| Diameter of bars (cm) | $\phi_{bar}$ | 2 |
| Surcharge load (kPa) | q | 12 |
| Backfill slope (degree) | $\beta$ | 0 |
| Internal friction angle of retained soil (degree) | $\phi$ | 36 |
| Internal friction angle of base soil(degree) | $\acute{\phi}$ | 0 |
| Unit weight of retained soil ($kN/m^3$) | $\acute{\gamma}_s$ | 18.86 |
| Unit weight of base concrete ($kN/m^3$) | $\gamma_c$ | 23.6 |
| Unit weight of soil ($kN/m^3$) | $\gamma_s$ | 17.3 |
| Cohesion of base soil (kPa) | c | 120 |
| Depth of soil in front of wall (m) | $D_f$ | 1.22 |
| Factor of safety for bearing capacity | $SF_b$ | 3 |
| Factor of safety against sliding | $SF_s$ | 1.5 |
| Factor of safety against overturning | $SF_o$ | 1.5 |

**Table 9**
Cost and weight optimum values for second verification case.

| Method | Objective function | value |
|---|---|---|
| Bowles (manual design) [9] | Cost ($/m) | 86.7692 |
| | Weight (kg/m) | 3543.6 |
| GBMOA algorithm | Cost ($/m) | 50.1979 |
| | Weight (kg/m) | 1943.8 |

**Table 10**
Optimum values of variables in optimum points for second verification case.

| Design parameters / Optimum value | | Cost | Weight |
|---|---|---|---|
| $X_1$ | Total base width (m) | 1.4194 | 1.4113 |
| $X_2$ | Toe width (m) | 0.355 | 0.355 |
| $X_3$ | Stem thickness at the bottom (m) | 0.2124 | 0.202 |
| $X_4$ | Thickness of base (m) | 0.2218 | 0.2218 |
| $X_5$ | Stem tensile steel area (m) | 5.4365 | 5.1843 |
| $X_6$ | Toe tensile steel area ($cm^2/m$) | 2.6399 | 1.3288 |
| $X_7$ | Heel tensile steel area ($cm^2/m$) | 5.5361 | 1.9232 |
| $X_8$ | Stem compressive steel area ($cm^2/m$) | 0 | 0 |
| $X_9$ | Toe compressive steel area ($cm^2/m$) | 0 | 0 |
| $X_{10}$ | Heel compressive steel area ($cm^2/m$) | 0 | 0 |
| $X_{11}$ | Yield strength of stem tensile steel (MPa) | 500 | 500 |
| $X_{12}$ | Yield strength of stem compressive steel (MPa) | 350 | 400 |
| $X_{13}$ | Yield strength of toe tensile steel (MPa) | 500 | 400 |
| $X_{14}$ | Yield strength of toe compressive steel (MPa) | 400 | 350 |
| $X_{15}$ | Yield strength of heel tensile steel (MPa) | 350 | 400 |
| $X_{16}$ | Yield strength of heel compressive steel (MPa) | 500 | 350 |
| $X_{17}$ | Compressive strength of Stem concrete (MPa) | 28 | 28 |
| $X_{18}$ | Compressive strength of base concrete (MPa) | 45 | 35 |
| $X_{19}$ | Diameter of bar (m) | 14 | 10 |
| $X_{20}$ | Number of stem tensile steel | 4 | 7 |
| $X_{21}$ | Number of toe tensile steel | 17 | 24 |
| $X_{22}$ | Number of heel tensile steel | 4 | 16 |
| $X_{23}$ | Number of stem compressive steel | 0 | 0 |
| $X_{24}$ | Number of toe compressive steel | 0 | 0 |
| $X_{25}$ | Number of heel compressive steel | 0 | 0 |

## 5. Parametric studies

To investigate the effect of the wall geometry on the weight and cost objective functions, four types for T-shape wall are considered (Figure 5). For these walls, primary parameters are selected as shown in Table 4. These walls are T-shape wall with varying stem thickness, normal T-shape wall, T-shape wall with two stem thicknesses, and T-shape wall with a thickness of stem and shear key. To increase the accuracy and consistency of comparisons between the geometry of the walls, the discrete variables are eliminated and their related values are considered constant based on Table 4. Moreover, all considered constraints in Table 3 are applied for all walls. The weight and cost objective functions for four different walls based on GBMOA algorithm are presented in Table 11.

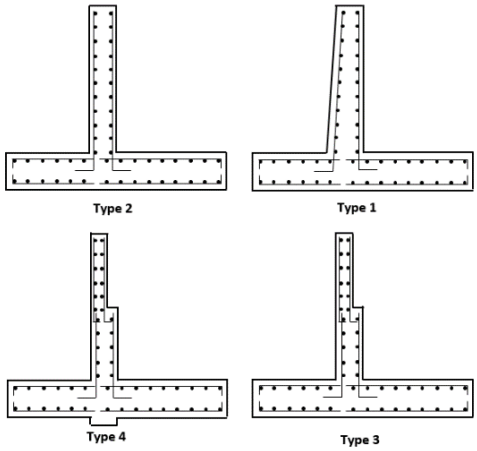


**Fig. 5.** Considered walls models for parametric studies.

**Table 11**
Values of objective functions for parametric studies.

| Objective function / Type of wall | Cost ($/m) | Weight (kg/m) |
|---|---|---|
| Type1 | 145.815 | 5013.64 |
| Type2 | 163.018 | 5461.8 |
| Type3 | 138.45 | 4801.15 |
| Type4 | 142.708 | 4961.93 |

The obtained results indicate that the normal T-shape wall has unsuitable performance due to greater weight and cost values than other types. The wall with two stem thicknesses has the lowest weight and cost values.

## 6. Sensitivity analysis

Some parameters contribute to the retaining wall optimization and thus the influence of each parameter on objective functions should be investigated. In this section, for sensitivity analyses, four types of walls (Figure 5) is considered with specifications presented in Table 4. As important influencing parameters on objective functions are backfill slope, surcharge, stem height and the backfill unit weight. It is noted that the backfill unit weight is assumed to be linearly proportional to its internal friction angle ($\phi$). For example, the backfill unit weight values of 15 and 18 $KN/m^3$ correspond to friction angle values of $30^o$ and $40^o$, respectively. The considered values for the mentioned parameters are summarized in Table 12.

**Table 12**
Parameters considered for sensitivity analysis.

| | parameter | symbol | value |
|---|---|---|---|
| 1 | Backfill slope (degree) | $\beta$ | $0^o$-$10^0$-$20^o$-$30^o$ |
| 2 | Height of stem (m) | $H_s$ | 3-4-5-6 |
| 3 | Surcharge (kPa) | q | 0-10-20-30-40 |
| 4 | Unit weight of retained soil ($kN/m^3$) | $\gamma_s$ | 15-16-17-18 |
| | Internal friction angle of soil (degree) | $\phi$ | 30-33.33-36.66-40 |

## 6.1. Effect of backfill slope

According to Figure 6, with increasing the backfill slope, the values of the cost and weight objective functions initially decrease and then increase. The results show that the minimum values for both objective functions are obtained for the slope angle of 20° and the maximum values are obtained for horizontal backfill. It is important to note that the maximum value of weight objective function for the second type of wall is obtained for β =30°. This is because the variation of objective functions shows that when the backfill slope increases, significant shear forces develop at the wall toe. The results show that the applied force to toe is affected by backfill slope and it can change the maximum and minimum of pressures ($q_{max}$, $q_{min}$). With increasing the backfill slope, $q_{max}$ decreases and $q_{min}$ increases. It should be noted that the variation of $q_{max}$ and $q_{min}$ values are effected on tension control constraint in the foundation. As an example, two backfill slope angles of 10° and 20° are considered and objective functions are computed. The results of the optimum point for the angle of 20° cannot gratify the constraints of the angle of 10°. This shows that the variation of the backfill slope affects tension control constraints.

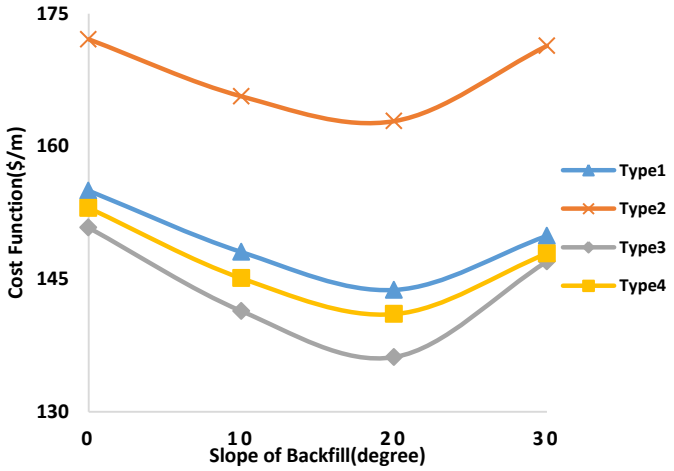


(a)

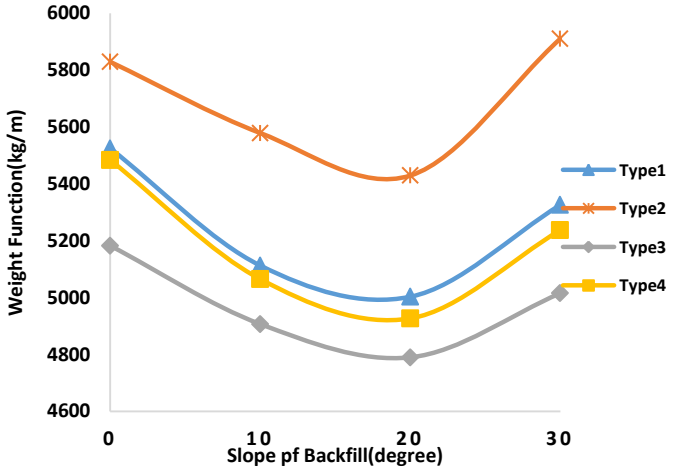


(b)

**Fig. 6.** Effect of increasing the backfill slope on: (a) cost objective function; (b) weight objective function.

## 6.2. Stem height

The effect of the stem height on the cost and weight functions is shown in Figure 7. As seen, with increasing the wall height, both functions increase. However, the rate of increase for the objective function is not equal for all four wall types. For example, when the stem height increases from 3 m to 4 m, the increase of the objective function is greater than when the stem height increases from 4 m to 5 m. It is important to note that the percentage increase decreases with increasing the wall height. Moreover, increasing the stem height has a higher influence on the cost objective function. In other words, the cost objective function has a higher increase percentage compared with weight objective function for all types of wall.

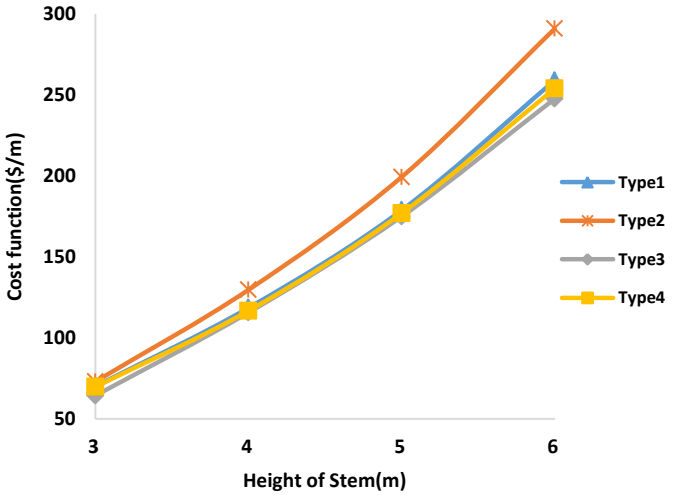


(a)

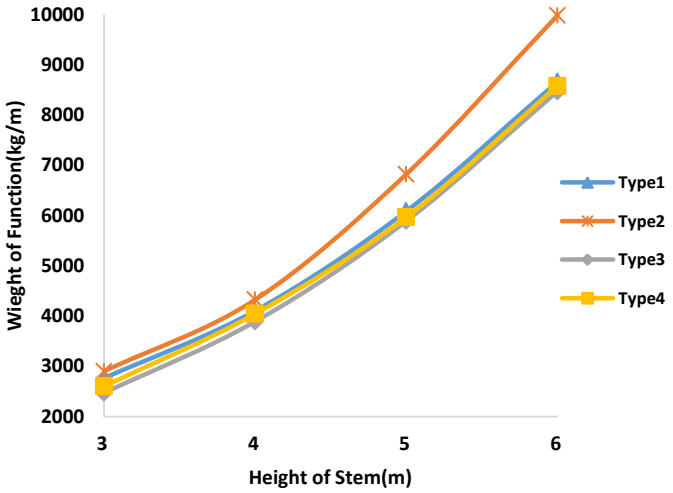


(b)

**Fig. 7.** The effect of increasing the height on the objective function values; (a) cost, (b) weight.

## 6.3. Effect of surcharge

The effect of surcharge on cost and weight functions is shown in Figure 8. As observed, with increasing the surcharge, cost and weight functions increase for all wall types. In addition, the increase of surcharge from 0 kPa to 40 kPa has higher influence on the cost objective function compared with weight objective function for all wall types. For example, the rate of increase for cost and weight objective functions for first type are %23.86 and %8.08, respectively. This means that the cost of wall has higher rate of increase. This was also found by Saribas and Erbatur (1996) [1].

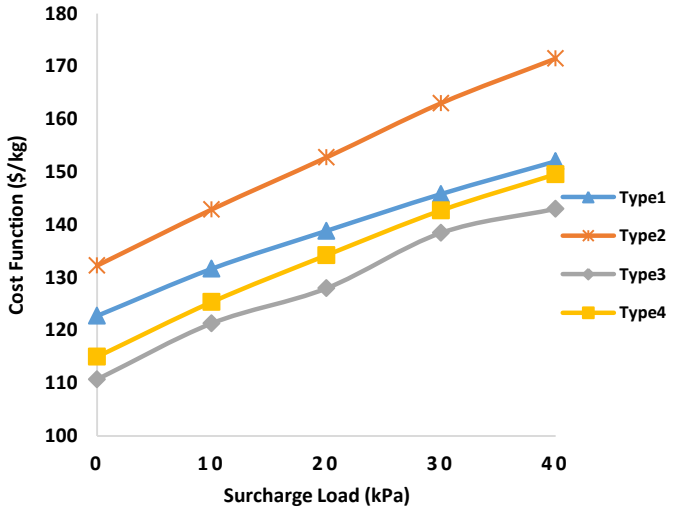


(a)

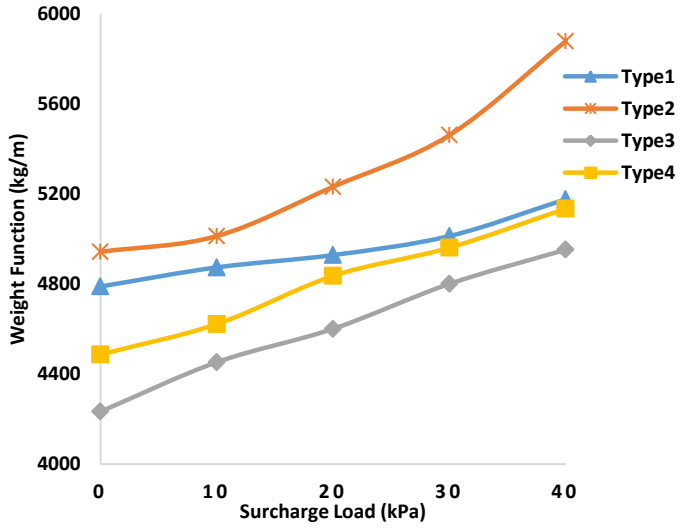


(b)

**Fig. 8.** Variation of objective functions with surcharge: (a) cost; (b) weight.

## 6.4. Unit weight and internal friction angle of soil

The effect of the soil unit weight ($\gamma_s$) and internal friction angle ($\phi$) of retained soil on cost and weight functions is shown in Figure 9. As illustrated, with $\gamma_s$ and $\phi$, both objective functions for all wall types obviously decrease. It should be noted that in Figure 9, the variations of objective functions are shown with $\gamma_s$. In other words, the horizontal axis consists of the values of $\gamma_s$ and $\phi$. For example, $\phi = 30^{\circ}$ for backfill corresponds to $\gamma_s = 15\ kN/m^3$, as previously mentioned. In addition, the reduction rate of cost and weight objective functions is not identical for all wall types. In addition, the reduction rate of functions is in the range of %15 to %20 for all wall types.

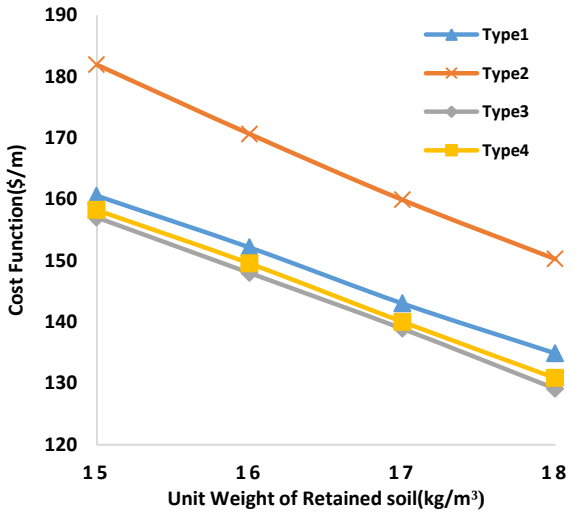


(a)

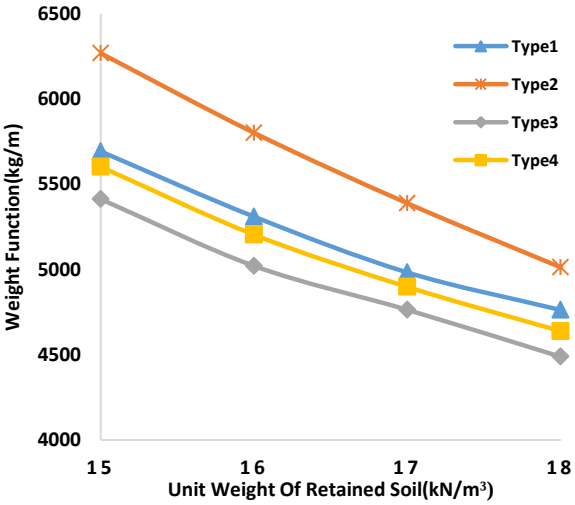


(b)

**Fig. 9.** Variation of objective function with backfill unit weight: (a) cost; (b) weight.

## 7. The effect of Coulomb and Rankine methods

To investigate the effect of lateral earth pressure theory on cost and weight objective functions, some T-shape walls having various stem thicknesses are considered. The results summarized in Table 13 indicate that two objective functions based on the Colomb theory are smaller than the Rankine one.

**Table 13**
Objective function values for Rankine and Coulomb earth pressure theories.

| Type of wall | Objective function / Method | Cost ($/m) | Weight (kg/m) |
|---|---|---|---|
| Type1 | Rankine | 145.815 | 5013.64 |
| | Coulomb | 139.87 | 4782.45 |
| Type2 | Rankine | 163.018 | 5461.8 |
| | Coulomb | 154.34 | 5101.56 |

## 8. Conclusions

This paper presents the application of the gasses Brownian motion algorithm (GBMOA) for optimization of reinforced concrete cantilever retaining walls. The results are compared with those available in the literature, resulting in the method capabilities. For this purpose, cost and weight objective functions are introduced and used for four types of T-shape walls. Sensitivity analyses have been performed to detect the influence of contributing parameters on the retaining wall optimization. It has been found that the wall cost and weight increase with increasing the wall stem height and surcharge. In addition, with increasing the backfill unit weight and internal friction angle, the cost and weight functions decrease. Moreover, with increasing the backfill slope angle, cost and weight objective functions initially decrease and then increase. Minimum objective functions are obtained for backfill slope angle of 20o. In addition, the use of Coulomb lateral earth pressure theory results in lower cost and weight objective functions than the Rankine theory.

## References

[1] Sarıbaş A, Erbatur F. Optimization and Sensitivity of Retaining Structures. J Geotech Eng 1996;122:649–56. doi:10.1061/(ASCE)0733-9410(1996)122:8(649).

[2] Sivakumar Babu GL, Basha BM. Optimum Design of Cantilever Retaining Walls Using Target Reliability Approach. Int J Geomech 2008;8:240–52. doi:10.1061/(ASCE)1532-3641(2008)8:4(240).

[3] Yepes V, Alcala J, Perea C, González-Vidosa F. A parametric study of optimum earth-retaining walls by simulated annealing. Eng Struct 2008;30:821–30. doi:10.1016/j.engstruct.2007.05.023.

[4] Ceranic B, Fryer C, Baines RW. An application of simulated annealing to the optimum design of reinforced concrete retaining structures. Comput Struct 2001;79:1569–81. doi:10.1016/S0045-7949(01)00037-2.

[5] Ghazavi M, Bazzazian Bonab S. Learning from ant society in optimizing concrete retaining walls. J Technol Educ 2011;5:205–12.

[6] Ghazavi M, Salavaty V. Sensitivity analysis and design and of reinforced concrete cantilever retaining walls using bacterial foraging optimization algorithm. Geotech Saf Risk ISGSR 2011 2011:307–14.

[7] Kaveh A, Behnam AF. Charged System Search Algorithm for the Optimum Cost Design of Reinforced Concrete Cantilever Retaining Walls. Arab J Sci Eng 2013;38:563–70. doi:10.1007/s13369-012-0332-0.

[8] Abdechiri M, Meybodi MR, Bahrami H. Gases Brownian Motion Optimization: an Algorithm for Optimization (GBMO). Appl Soft Comput 2013;13:2932–46. doi:10.1016/j.asoc.2012.03.068.

[9] Bowles LE. Foundation analysis and design. McGraw-hill; 1982.

[10] Committee ACI, Standardization IO for. Building code requirements for structural concrete (ACI 318-08) and commentary, American Concrete Institute; 2008.